Amino Acids (2015) 47:949–961
DOI 10.1007/s00726-015-1924-2

ORIGINAL ARTICLE

Pacific oyster polyamine oxidase: a protein missing link in invertebrate evolution

Manuela Cervelli · Fabio Polticelli · Emanuela Angelucci · Elena Di Muzio · Pasquale Stano · Paolo Mariottini

Received: 12 November 2014 / Accepted: 15 January 2015 / Published online: 6 February 2015

Abstract Polyamine oxidases catalyse the oxidation of polyamines and acetylpolyamines and are responsible for the polyamine interconversion metabolism in animal cells. Polyamine oxidases from yeast can oxidize spermine, N^1-acetylspermine, and N^1-acetylspermidine, while in vertebrates two different enzymes, namely spermine oxidase and acetylpolyamine oxidase, specifically catalyse the oxidation of spermine, and N^1-acetylspermine/N^1-acetylspermidine, respectively. In this work we proved that the specialized vertebrate spermine and acetylpolyamine oxidases have arisen from an ancestor invertebrate polyamine oxidase with lower specificity for polyamine substrates, as demonstrated by the enzymatic activity of the mollusc polyamine oxidase characterized here. This is the first report of an invertebrate polyamine oxidase, the Pacific oyster *Crassostrea gigas* (CgiPAO), overexpressed as a recombinant protein. This enzyme was biochemically characterized and demonstrated to be able to oxidase both N^1-acetylspermine and spermine, albeit with different efficiency. Circular dichroism analysis gave an estimation of the secondary structure content and modelling of the three-dimensional structure of this protein and docking studies highlighted active site features. The availability of this pluripotent enzyme can have applications in crystallographic studies and pharmaceutical biotechnologies, including anticancer therapy as a source of hydrogen peroxide able to induce cancer cell death.

Keywords Polyamine oxidase · Pacific oyster · Enzyme activity · Tertiary structure

Abbreviations

AcSpd	N^1-acetylspermidine
AcSpm	N^1-acetylspermine
APAO	N^1-acetylpolyamine oxidase
CgiPAO	*Crassostrea gigas* polyamine oxidase
FAD	Flavin adenine dinucleotide

Handling Editor: S. Beninati.

Electronic supplementary material The online version of this article (doi:10.1007/s00726-015-1924-2) contains supplementary material, which is available to authorized users.

M. Cervelli (✉) · F. Polticelli · E. Angelucci · E. Di Muzio · P. Stano · P. Mariottini
Department of Sciences, University of Roma Tre, 00146 Rome, Italy
e-mail: manuela.cervelli@uniroma3.it

F. Polticelli
e-mail: polticel@uniroma3.it

E. Angelucci
e-mail: emanuela.angelucci@uniroma3.it

E. Di Muzio
e-mail: elena.dimuzio@uniroma3.it

P. Stano
e-mail: pasquale.stano@uniroma3.it

P. Mariottini
e-mail: paolo.mariottini@uniroma3.it

M. Cervelli · P. Mariottini
Interuniversity Consortium of Structural and Systems Biology, 00136 Rome, Italy

F. Polticelli
National Institute of Nuclear Physics, Roma Tre Section, 00146 Rome, Italy

FMN	Flavin mononucleotide
H_2O_2	Hydrogen peroxide
PAO	Polyamine oxidase
PAs	Polyamines
Put	Putrescine
Spd	Spermidine
Spm	Spermine
SMO	Spermine oxidase
ZmPAO	Maize polyamine oxidase

Introduction

Polyamine oxidases (PAOs) are flavin adenine dinucleotide (FAD)-containing enzymes that catalyse the oxidation of polyamines (PAs) at the secondary amino group, thereby giving different products according to the organism considered. Vertebrate acetylpolyamine oxidases (APAOs, EC 1.5.3.11) participate in the interconversion metabolism of PAs, converting N^1-acetyl derivatives of spermine (Spm) and spermidine (Spd) into Spd and putrescine (Put), respectively, plus 3-acetamidopropanal and hydrogen peroxide (H_2O_2) (McIntire and Hartman 1993; Van den Munckhof et al. 1995; Cervelli et al. 2003, 2004; Bellelli et al. 2004). On the other hand, in vertebrates, Spm is directly oxidized by the enzyme spermine oxidase (SMO, EC 1.5.3.16), a well-characterized flavoprotein (Cervelli et al. 2003, 2013a), and Spm oxidation leads to the production of Spd, 3-aminopropanal and H_2O_2. In the last decades, these PA catabolic enzymes have been extensively characterized and it is well documented that both oxidases play an essential role in maintaining vertebrate PA homeostasis, which is mandatory for cellular life, and their dysregulation is associated with pathological diseases (Thomas and Thomas 2001; Agostinelli et al. 2004; Casero and Marton 2007; Amendola et al. 2009, 2014; Cervelli et al. 2010, 2013a, b, 2014a; Capone et al. 2013). Modelling studies of mouse APAO (Bianchi et al. 2006) and SMO (Bianchi et al. 2005; Cervelli et al. 2003; Tavladoraki et al. 2011) enzymes have indicated a very similar active site environment for the two proteins, making it difficult to rationalize their different substrate specificity (Cervelli et al. 2012, 2014b). The biochemical characterization and the crystal structure analysis of the *Saccharomyces cerevisiae* enzyme Fms1 have demonstrated that this PAO is able to oxidize Spm, N^1-acetylSpm (AcSpm) and N^1-acetylSpd (AcSpd) (Landry and Sternglanz 2003; Huang et al. 2005). The molecular evolutionary history of this gene family has been described in Metazoa (Polticelli et al. 2012). It was proposed that the biochemical function of invertebrate enzymes, able to catalyse the oxidation of both acetylated and non-acetylated polyamines, is accomplished in vertebrates by the two specialized polyamine oxidases APAO and SMO, which are derived from the ancestral invertebrate enzyme (Polticelli et al. 2012). In this study we report the cloning and biochemical characterization of the invertebrate PAO enzyme from the Pacific oyster (*Crassostrea gigas*), named CgiPAO, capable of oxidizing AcSpm and Spm. In particular, the recombinant enzyme was expressed in a tagged form into *Escherichia coli* BL21 DE3 cells. The purified recombinant enzyme displays K_m and k_{cat} values that corroborate this view. Molecular modelling of the CgiPAO protein highlights active site features shared with other structurally characterized PAOS and support the hypothesis that the specialized vertebrate APAOs and SMOs have arisen from less substrate-specific invertebrate PAOs.

Materials and methods

Protein sequence homology search and phylogenetic analysis

Full-length PAO protein sequences were retrieved from public databases (UniProt, http://www.ebi.ac.uk/uniprot/ PFAM, http://www.sanger.ac.uk/Sofware/Pfam/ and GenBank http://www.ncbi.nlm.nih.gov/). Whenever possible, sequences whose enzymatic activities had been previously verified have been used as query sequences in BLAST searches. Blastp scoring parameters were the following: max target sequences: 100; short queries: automatically adjust parameters for short input sequences; expected threshold: 10; word size: 3; max matches in a query range: 0; matrix: BLOSUM62; gap costs: existence: 11, extension: 1; compositional adjustments: conditional compositional score matrix adjustment. Additional predicted invertebrate PAO and plant protein sequences were retrieved from currently sequenced and unfinished genomes at the Ensembl database (http://www.ensembl.org/index.html). Multiple amino acidic sequences alignment was performed using CLUSTALW (Larkin et al. 2007). Phylogenetic analyses were performed by the Maximum Likelihood and the Bayesian inference methods using plant PAOs as outgroup. Maximum Likelihood analysis was carried out in PALM (Chen et al. 2009). The JTT model with a proportion of invariable sites (I) and gamma-distributed rates across sites (G) was selected for the phylogenetic inference. Nodes support for the resulting phylogenetic tree was evaluated by 1,000 mL bootstrap replications. Bayesian inference analysis was performed with MrBayes 3.2 (Ronquist et al. 2012) under the same model of protein evolution [two independent runs of four Markov chain Monte Carlo (MCMC) chains for 1 million generations each, sampling every 100 generations, and posterior probabilities for nodes derived from a majority rule consensus of the trees sampled after convergence (25 % was sett as burn-in for sumt and sump).

Chemicals and DNA methodology

Spm and Spd were purchased from Sigma; **AcSpm** originally purchased from Sigma is no longer commercially available. The methods described by Sambrook et al. (1989) were used for the extraction and manipulation of plasmid DNA and general DNA in vitro methods. Nucleotide sequencing was carried out for both strands using the automated fluorescent dye terminator technique (Perkin Elmer ABI model 373A).

Construction of pCgiSMO-HT expression plasmid

The Pacific oyster CgiPAO cDNA sequence was deduced from the corresponding gene (GenBank accession number EKC38899) (Zhang et al. 2012). For the CgiPAO cDNA synthesis, total RNA was purified, using TRIzol reagent (Gibco BRL) according to the manufacturer's instructions, from the mantle membrane of a *C. gigas* specimen collected from the Tyrrhenian Sea and then used for RT-PCR. Synthesis of the specific cDNA was obtained using the primer CgiPAO-REV (5′-ACGTTTAGTCTGAGTACAGTTTG-3′) and the SuperScript III First-Strand (Invitrogen) according to the manufacturer's instructions. Full-length CgiPAO cDNA synthesis was obtained from the first-strand cDNA using as primers two oligonucleotides designed to introduce *Nde*I and *Xho*I restriction sites at the 5′ and 3′ ends: CgiPAO-FOR (5′-CATATGGGCGAAAAAGTGATAGATG-3′) and CgiPAO-HT-REV (5′-AAATATCTCGAGTCAATGAT GATGATGATGATGGTCTGAGTACAGTTTG-3′), respectively. The amplified PCR product was restricted with *Nde*I and *Xho*I and ligated with the restricted *Nde*I/*Xho*I pET17b vector (Novagen), to obtain the genetic construct named pCgiPAO-HT containing the mature form of CgiPAO protein joined to a C-terminal 6xHisTAG. The recombinant cDNA construct was sequenced to check the accuracy of the nucleotide sequence and then used to transform *E. coli* BL21 DE3 (Novagen) competent cells.

Expression of CgiPAO in *E. coli* cells

Escherichia coli BL21 DE3 cells transformed with the pCgiPAO-HT plasmid were grown at 30 °C in LB medium containing 100 μg/mL ampicillin to $A_{660} = 0.6$ and then induced with isopropyl-β-D-thiogalactopyranoside (1 mM final concentration), followed by further cultivation for 5 h at 28 °C. The *E. coli* BL21 DE3 cells were harvested by centrifugation (4 °C, 10 min, 10,000*g*), washed with 0.4 volume/culture weight of 30 mM Tris–HCl (pH 8.0), containing 20 % sucrose and 1 mM EDTA, and incubated 5–10 min at room temperature. The suspension was then centrifuged (10,000*g* for 10 min at 4 °C) and the cell pellet stored at −20 °C until use.

Rapid affinity purification with pET His Tag systems

Cell pellet was resuspended in 5 mM imidazole, 0.5 M NaCl, 10 % glycerol, 20 mM Tris–HCl (pH 7.9) and then sonicated. After centrifugation (12,000*g* for 30 min at 4 °C) the soluble cell extract was purified by the His-Bind chromatography kit (Novagen). In particular, the supernatant was applied to a column (3 mL) with Ni^{2+} cations immobilized on the His-Bind resin (Novagen), equilibrated with the binding buffer (5 mM imidazole, 0.5 M NaCl, 10 % glycerol, 20 mM Tris–HCl, pH 7.9). The column was washed with binding buffer and then elution was performed with 500 mM imidazole, 0.5 M NaCl, 10 % glycerol, 20 mM Tris–HCl (pH 7.9). SDS/PAGE electrophoretic analysis was performed on the purified recombinant CgiPAO tagged protein to assess the purity grade.

Absorption and fluorescence spectroscopy

Absorption spectra were measured by an Agilent 8453 diode-array spectrophotometer using a 1 cm quartz microcuvette (sample volume 80 μL). Excitation and emission spectra were recorded by a Jasco FP-6200 fluorimeter, using a 0.3 cm quartz microcuvette (sample volume 60 μL), with the following instrumental settings: excitation wavelength: 450 nm, emission wavelength: 530 nm, excitation and emission slits: 5 nm, scan rate: 250 nm/min, sensitivity: high. Fluorescence spectra were recorded at a protein concentration of 2.5 μM. All measurements were carried out in 0.1 M Tris–HCl (pH 8.5) at 25.0 °C.

Cofactor analysis

Purified recombinant CgiPAO was denatured by boiling for 15 min in the dark. The denatured protein was removed by centrifugation and the excitation/emission spectra of the supernatant were recorded before and after 15×10^{-3} U/mL of phosphodiesterase (PDE) treatment [which converts FAD to flavin mononucleotide (FMN)]. Once determined the chemical nature of the cofactor (FAD), the protein concentration was evaluated spectrophotometrically using a molar extinction coefficient ε_{450} of 10,000 cm^{-1} M^{-1}.

Circular dichroism (CD)

CD spectra of CgiPAO in 5 mM Tris–HCl (pH 8.5) were recorded at 25.0 °C using a Jasco J-600 spectropolarimeter and cylindrical quartz cells having 0.05 cm (far UV) or 0.5 cm (near UV/Vis) path length. Protein concentration was calculated spectrophotometrically, and resulted to be 1 and 100 μM (i.e. 55 and 5,500 μg/mL) for far-UV and near-UV/Vis analyses, respectively. Instrumental

ellipticity θ (mdeg) was converted to mean molar ellipticity $[\theta]$ (deg cm^2/dmol) and $\Delta\varepsilon$ (cm^{-1} M^{-1}) by taking into account the cell path length and the protein concentration. For each sample, sixteen CD spectra in the far-UV region (190–240 nm) and four in the near-UV/Vis region (300–550 nm) were recorded, averaged and smoothed. Spectra are shown in terms of $\Delta\varepsilon$ per residue in the far-UV region and $[\theta]_{FAD}$ in the near-UV/Vis region. Estimation of the secondary structure content was carried out using Dicroprot2000 (Deleage and Geourjon 1993) and CD-PRO (Sreerama and Woody 2000) software packages, according to the K2D neural network algorithm (Andrade et al. 1993).

CgiPAO catalytic activity assay and determination of the kinetic constants

Enzyme activity was measured spectrophotometrically by following the formation of a pink adduct ($\varepsilon_{515} = 2.6 \times 10^4$ M^{-1} cm^{-1}) as a result of the oxidation and following condensation of aminoantipyrine and 3,5-dichloro-2-hydroxybenzenesulfonic acid, catalysed by horseradish peroxidase (Polticelli et al. 2005). Measurements were performed in 0.1 M Tris–HCl buffer (pH 8.5), with substrates at various concentrations. In the enzyme assays the CgiPAO concentration was in the range of 1.0–5.0 μM. k_{cat} values were calculated using saturating concentrations of AcSpm (2 mM) and Spm (4 mM) and keeping the O_2 concentration constant at the air-saturated level (ca. 300 μM). The K_m and V_{max} values for AcSpm and Spm were determined by Lineweaver–Burk plots; fitting of the data was performed using the GraphPad Prism 4.0 software. Studies of the pH dependence of CgiPAO activity were conducted in 0.1 M Tris–HCl buffer (pH range values from 6.5 to and 9.0), and in 0.1 M sodium borate buffer (pH range values from 8.5 to 10.0) at 25 °C using saturating concentrations of both substrates. Data reported in the Results section are the average of at least three independent experiments carried out in duplicates. Enzyme activities were expressed in International Units (IU: the enzyme amount catalysing the oxidation of 1 μmol of substrate/min) per litre of culture broth. Catalytic activity of CgiPAO was negligible using Spd as substrate. When needed, protein content was estimated by the method of Bradford (1976) with bovine serum albumin as a standard. Purity was assayed by SDS-PAGE, according to the method of Laemmli (1970).

Modelling of the three-dimensional structure of CgiPAO and docking studies

The molecular model of CgiPAO was built using the pipeline implemented in the ab initio molecular modelling package I-TASSER which has been shown to yield reliable results in a number of different studies (see Xu et al. 2011 and references therein). I-TASSER first retrieves template proteins which are predicted to display a fold similar to the protein of interest, using several different threading approaches implemented in LOMETS (FUGUE, HHsearch, MUSTER, PPA, PROSPECT2, SAM-T02, SPARKS, SP3, FFAS and PRC). Subsequently, structure fragments excised from the templates are reassembled by replica-exchange Monte Carlo simulations and models are refined in an iterative procedure that optimizes the free energy and the global topology of the models (Roy et al. 2010). The best templates identified by I-TASSER were a FAD-dependent oxidoreductase from *Arthrobacter aurescens* (PDB code 3RHA; to be published) and *Zea mays* PAO (PDB code 1B5Q; Binda et al. 1999). Docking simulations of AcSpm and Spm into the active site of CgiPAO were performed using Autodock Vina (Trott and Olson 2010), allowing flexibility of the active site residues selected by comparison of CgiPAO structural model with the three-dimensional structure of the Fms1–Spm complex (PDB code 1XPQ; Huang et al. 2005). The water molecule bridging the FAD cofactor to the catalytically essential Lys residue (Polticelli et al. 2005; Tavladoraki et al. 2011), Lys315 in CgiPAO, was explicitly included in the docking simulations.

Results

Phylogeny of the invertebrate polyamine oxidase family

A BLASTP search of invertebrate PAO homologs carried out in the available databases (see "Materials and methods" section for details), retrieved 29 sequences annotated as PAO proteins from plants, baker's yeast (*Saccharomyces cerevisiae*) and invertebrate taxa, including Placozoa (*Trichoplax adhaerens*), Cnidaria, Echinodermata, Mollusca, Annelida, Arthropoda, Nematoda and Chordata (Table 1). The PAO protein sequence from the gastropod *Colubraria reticulata* was derived from the unpublished transcriptome of this species, currently under study (Oliverio and Modica, personal communication). Multiple amino acid sequence alignment of PAO proteins highlighted a fairly good degree of sequence similarity (Fig. 1). The evolutionary tree (Fig. 2) was coherent with the phylogenetic reconstruction of the invertebrate PAOs proposed by Polticelli et al. (2012). In particular, the oyster *C. gigas* PAO which belongs to a lophotrochozoan clade was nested in a molluscan lineage and shared with the mollusc PAOs an identity of 66 % (*Lottia gigantean*, ESO98426), 58 % (*Colubraria reticulata* Oliverio and Modica) and 55 % (*Aplysia californica*, 005092230), while shared with the Anellida

Table 1 Polyamine oxidase proteins sequences included in the phylogenetic analyses and their corresponding accession numbers

Organism and acronym	Accession number
Metazoa	
Acromyrmex echinatior Panamanian leafcutter ant (Aec)	[EGI59478]
Anopheles gambia malaria mosquito (Aga)	[XP_312316.3]
Apis florea little honeybee (Afl)	[XP_003691813]
Apis mellifera honeybee (Ame)	[XP_001122522]
Aplysia californica Califonia sea hare (Aca)	[XP_005092230]
Camponotus floridanus Florida carpenter ant (Cfl)	[EFN70585]
Capitella teneta marine polychaete worm (Cte)	[ELT94559]
Ciona intestinalis sea squirt (Cin)	[XP_002132119]
Crassostrea gigas Pacific oyster (Cgi)	[EKC38899]
Colubraria reticulata sea gastropod (Cre)	[Oliverio and Modica, pers. com]
Dendroctonus ponderosae mountain pine beetle (Dpo)	[478251226]
Drosophila melanogaster fruit fly (Dme)	[Q9VHN8]
Harpegnathos saltator Jerdon's jumping ant (Hsa)	[EFN82405]
Helobdella robusta freshwater leech (Hro)	[ESO00558]
Lottia gigantea owl limpet (Lgi)	[ESO98426]
Megachile rotundata alfalfa leafcutting bee (Mro)	[XP_003699937]
Nasonia vitripennis jewel wasp (Nvi)	[XP_001599761]
Nematostella vectensis starlet sea anemone (Nve)	[XP_001637328]
Pediculus humanus corporis human body louse (Phu)	[EEB13427]
Solenopsis invicta red fire ant (Sin)	[EFZ20860]
Strongylocentrotus purpuratus purple urchin (Spu)	[XP_001195328]
Tribolium castaneum red flour beetle (Tca)	[XP_971067]
Trichoplax adhaerens tablet animal-Placozoa (Tad)	[XP_002107802]
Plants	
Arabidopsis thaliana (Ath1)	[NP_196874]
Hordeum vulgare	
(Hvu1)	[Q93WM8]
(Hvu2)	[Q93WC0]
Zea mays (Zma)	[NP_001105106]
Fungi	
Saccharomyces cerevisiae baker's yeast (FMS1)	[YDL174C]

PAOs an identity of 48 % (*Capitella tenella*, ELT94559) and 43 % (*Helobdella robusta*, ESO00558).

Heterologous expression and protein purification of CgiPAO

The CgiPAO cDNA clone was obtained as described in the Methods section. The recombinant cDNA construct pCgiPAO-HT (secreted-tagged form) was used to transform *E. coli* BL21 DE3 cells. After induction with IPTG, under the control of the T7 promoter, the catalytically active protein was expressed at a level of about 1.0 IU/litre of culture broth. The recombinant CgiPAO protein was purified (see "Materials and methods" section) and assayed by SDS/PAGE electrophoretic analysis, resulting in a single band of 55 kDa (Fig. 3).

Spectroscopic characterization of CgiPAO

The absorption spectrum of the native enzyme CgiPAO showed two peaks in the near-UV/Vis region, typical of oxidized flavoproteins, as previously described for animal SMO by Cervelli et al. (2003), with maxima at 365 and 450 nm (Fig. 4a). Being the first time, to the best of our knowledge, that a polyamine oxidase from *C. gigas* has been purified, the chemical nature of the flavin cofactor was first verified. The identity of the cofactor was determined by fluorescence analysis, according to the method described by Aliverti et al. (1999). The method exploits the fact that the fluorescence of a FMN solution is about tenfold higher than that of a FAD solution. The excitation and the emission spectra of (a) native recombinant CgiPAO, was obtained after purification; (b) supernatant

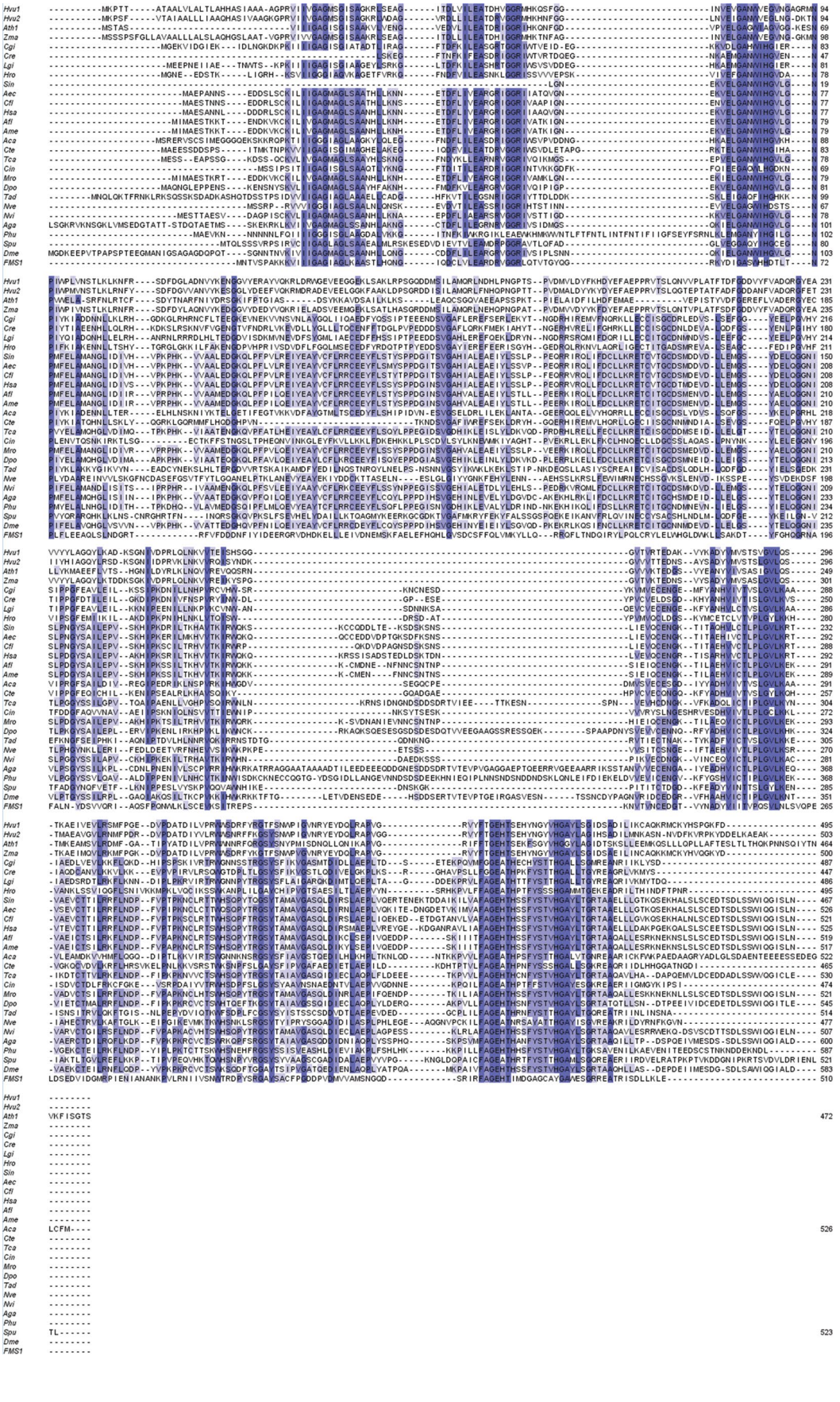
Hvu1
Hvu2
Ath1
Zma
Cgi
Cre
Lgi
Hro
Sln
Aec
Ctl
Hsa
Atf
Ame
Aca
Cte
Tca
Cin
Mro
Dpo
Tad
Nve
Nvi
Aga
Phu
Spu
Dme
FMS1

◀**Fig. 1** Multiple amino acid sequence alignment of polyamine oxidase proteins. The analysis involved 29 amino acidic sequences. Sequence blocks are coloured from *light* to *dark blue* according to increasing conservation score. Sequence-specific numbering is given on the *right end side* of the figure. The alignment was obtained using CLUSTALW2 (Larkin et al. 2007) and visualized using JalView (Waterhouse et al. 2009) (colour figure online)

was obtained after heat denaturation; and (c) supernatant after treatment with phosphodiesterase (15×10^{-3} U/mL) are shown in Fig. 4b. The very low fluorescence of the CgiPAO-bound cofactor (F_{530} ~6 a.u.) increased when the free cofactor was released after protein denaturation (F_{530} ~32 a.u.). Next, the addition of phosphodiesterase led to a strong fluorescence increase following FAD hydrolysis, to give FMN (F_{530} ~350 a.u.). The latter increase demonstrated that FAD was the CgiPAO flavin cofactor. Circular dichroism (CD) was employed to characterize the structure of CgiPAO in the near-UV/Vis and in the far-UV regions. The near-UV/Vis CD spectrum in the FAD region was analysed and compared with the spectrum of the well-known mouse SMO, for which a structural model is available (Tavladoraki et al. 2011; Cervelli et al. 2013a, b, 2014b), evidencing several similarities. In particular, the spectrum (Fig. 4c) was characterized by several valleys and peaks, which revealed underlying individual transitions (Edmonson and Tollin 1971). Two valleys at 308 and 353 nm were evident, but also two peaks at 324 and 447 nm were present. However, the peaks displayed several shoulders. By comparison, the values for valley and peaks in the mouse SMO FAD spectrum were 304 and 352 nm, and 320 and 461 nm, respectively. This very similar spectral pattern suggested that FAD molecular microenvironment in CgiPAO and in mouse SMO was similar. The far-UV CD spectrum showed the typical shape of a well-folded protein, with a broad negative band between 205 and 225 nm and a positive peak centred around 192 nm (Fig. 4d). The deconvolution of the CD spectrum gave an estimate of α-helix and β-sheet content of about 38 and 15 %, which was in a quite satisfactory agreement with the values obtained by structural modelling (28 and 13 %, respectively), see below.

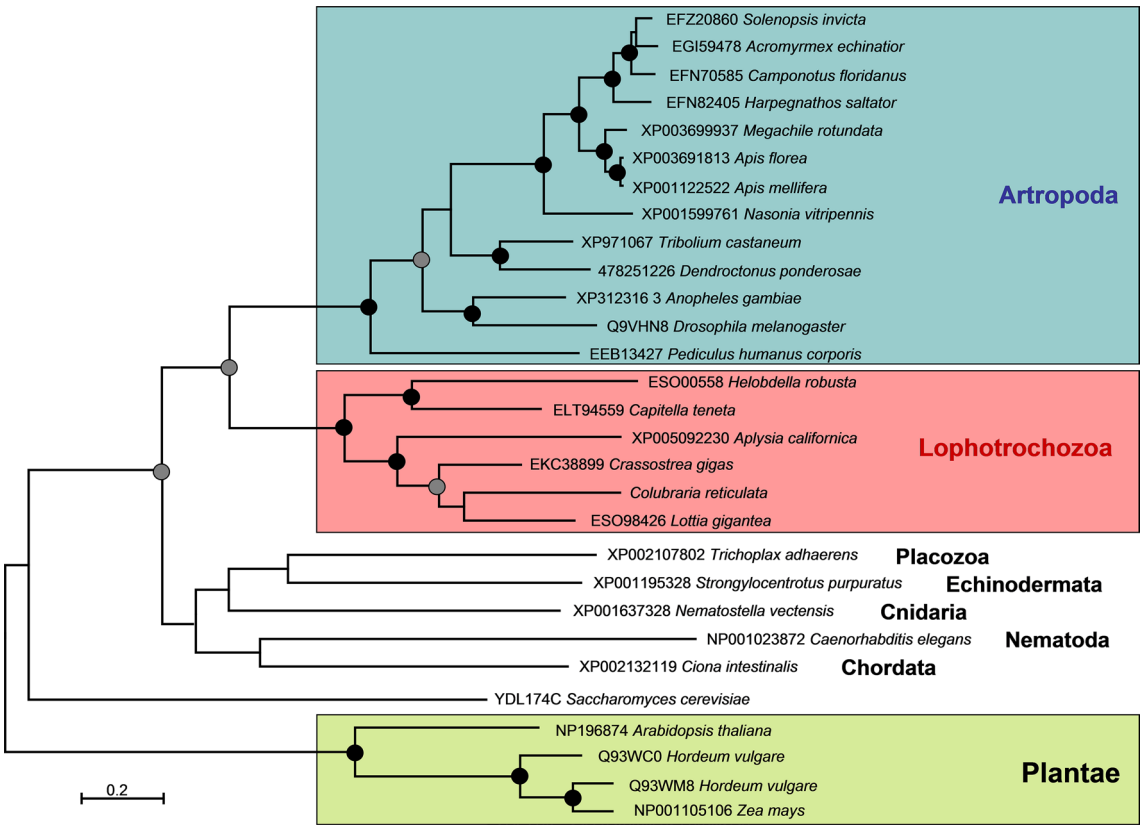

Fig. 2 The evolutionary tree of the invertebrate polyamine oxidase proteins. The evolutionary history tree of the polyamine oxidase proteins was inferred using the Maximum Likelihood method (log likelihood = −21985.9337) based on the JTT model with a proportion of invariable sites (I) and gamma-distributed rates across sites (G) (Bayesian tree showed identical topology at the main nodes; data not shown). The analysis involved 29 amino acidic sequences, and the tree was rooted with the plant sequences as outgroup. In correspondence of the nodes the bootstrap support (BS) and Bayesian posterior probabilities (BPP) are indicated by *black circles* (BS ranging from 95 to 100; BPP = 1.00) and *grey circles* (BS ranging from 90 to 94; BPP ranging from 0.95 to 0.99). The scale for branch lengths was measured by the number of substitutions per site

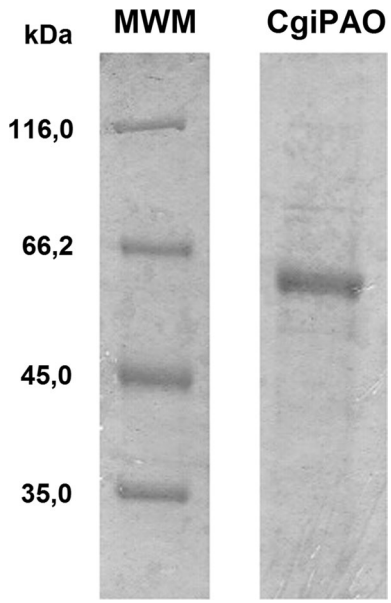

Fig. 3 Purified recombinant CgiPAO. SDS-PAGE analysis of the recombinant protein (3 μg of the purified enzyme), after Coomassie blue-brilliant staining. *MWM* molecular weight marker (Protein Molecular Weight Thermo)

Kinetic properties of CgiPAO

The purified CgiPAO exhibited a pH optimum of 8.5 in 0.1 M Tris–HCl buffer (see "Materials and methods" section). The enzyme activity at pH 7.5 and 9.5 resulted to be 40 and 45 % of the maximum for AcSpm, while for Spm resulted to be 35 and 40 % of the maximum (data not shown). The substrate specificity of CgiPAO for AcSpm and Spm was then investigated under standard conditions at pH 8.5. The purified enzyme oxidizes rapidly AcSpm and less efficiently Spm. The kinetic parameters of the tagged recombinant enzyme for AcSpm and Spm oxidation were also determined at pH 8.5. The values of K_m and k_{cat} resulted to be 33 (±1.0) μM and 19.0 (±0.6) × 10^{-3}/s, respectively, using AcSpm as a substrate, and 4.4 (±1.1) × 10^3 μM and 4.6 (±1.2) × 10^{-3}/s^{-1}, respectively, using Spm (Table 2; Fig. S1). The catalytic efficiency k_{cat}/K_m values was 576 and 1.0 s^{-1} M^{-1} for AcSpm and Spm, respectively, indicating that AcSpm was the preferred substrate for CgiPAO, although this difference is mainly due to K_m rather than k_{cat} values (Table 2).

Structural features of CgiPAO structural model

The primary structure of CgiPAO was deduced from the cDNA sequence, and its open reading frame predicts a 487-aminoacid protein with a theoretical pI of 5.21 and a MW of 55,148 Da. A structural model of CgiPAO was built using the pipeline implemented in the ab initio molecular modelling package I-TASSER (Roy et al. 2010; Xu et al. 2011; see "Materials and methods" section for details). The best templates identified by I-TASSER were a FAD-dependent oxidoreductase from *Arthrobacter aurescens* (PDB code 3RHA) and *Zea mays* PAO (PDB code 1B5Q). The top panel of Fig. 5 shows a schematic representation of CgiPAO model compared to the three-dimensional structures of yeast PAO Fms1 (PDB code 1XPQ; Huang et al. 2005) and *Zea mays* PAO (ZmaPAO; PDB code 1B5Q; Binda et al. 1999). It must be remarked that these crystal structures are the only structures available for members of the PAO family. As it can be seen, the overall fold of CgiPAO was typical of PAOs, with a FAD-binding domain and a substrate-binding domain. Analysis of the secondary structure content of the CgiPAO molecular model revealed that, out of 487 residues, 138 (28 %) are in α-helix conformation and 61 (13 %) in β-sheet conformation, percentage values which were in good agreement with those derived from the fitting of circular dichroism spectroscopy data. The FAD molecular environment was well conserved with respect to both Fms1 and ZmPAO. However, as it can be seen in the bottom panel of Fig. 5, CgiPAO active site composition is more similar to that of Fms1 than that of ZmPAO. In particular CgiPAO displayed the presence of His78 and Tyr423, conserved in Fms1 as His67 and Tyr450 while substituted in ZmPAO as Glu62 and Phe403.

Molecular docking of AcSpm and Spm into CgiPAO active site

In Fig. 6 is shown a schematic representation of the complexes formed by CgiPAO with AcSpm and Spm obtained by docking simulations. The two substrates bind in a similar fashion within the active site. In particular, in the CgiPAO–AcSpm complex the substrate forms hydrophobic interactions with Tyr423 and establishes hydrogen bonds with the FAD N5 atom, with the carbonyl oxygen atoms of Cys189 and Ser465, and with the side chain hydroxyl group of Ser465. In the CgiPAO–Spm complex the substrate forms hydrophobic interactions with Tyr423 and establishes hydrogen bonds with the FAD-bound water molecule, with the carbonyl oxygen atoms of Cys189, Ser465 and Thr466, and with the side chain hydroxyl group of Ser465. The substrate C4 atom which is oxidized during the catalytic reaction (the carbon atom in *eso* with respect to the secondary amino group of the substrate) is located at a 3.7 and 5.9 Å distance from the redox active N5 atom of FAD in the CgiPAO–AcSpm and the CgiPAO–Spm complex, respectively. Docking simulations correctly rank the two substrates and the binding energy values, calculated using the semi-empirical AutoDock force field (Trott and Olson 2010), are −6.6 and −5.7 kcal/mol for AcSpm and Spm complex, respectively, therefore, being in agreement with the lower K_m values determined for AcSpm.

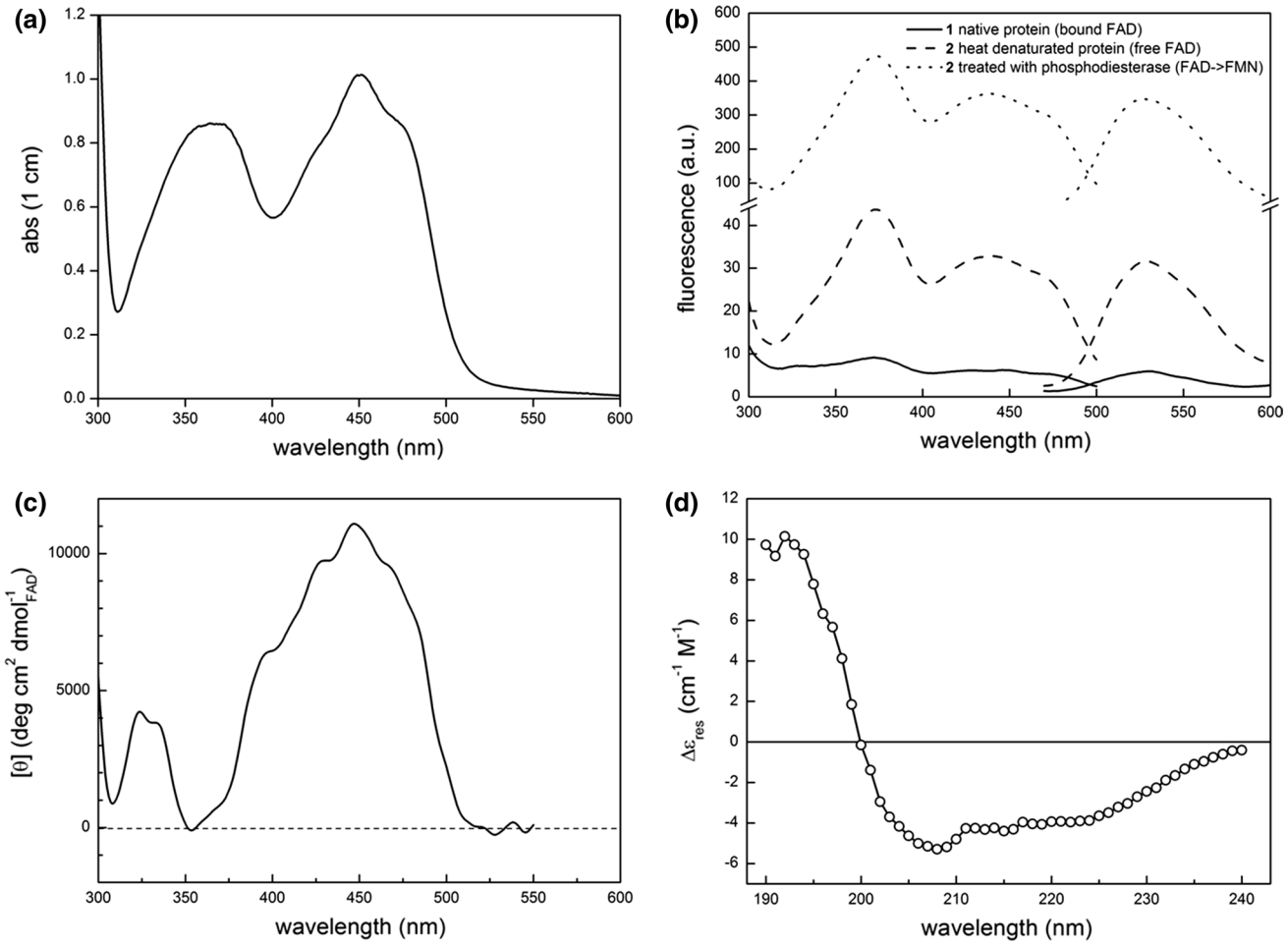

Fig. 4 Spectroscopic characterization of CgiPAO. **a** Absorption spectrum of CgiPAO (100 μM) in the near-UV/Vis region. **b** Fluorescence excitation (*curves* on the *left*) and emission spectra (*curves* on the *right*) of recombinant CgiPAO. Spectra 1 (*continuous lines*) were recorded under native conditions (whereby FAD is bound to the protein, therefore, quenched). Spectra 2 (*dashed lines*) refers to supernatant obtained after denaturation by boiling and centrifugation (released FAD, unquenched). Spectra 3 (*dotted lines*) were recorded after the treatment of supernatants with phosphodiesterase, that converts FAD in FMN, with further fluorescence enhancement (Aliverti et al. 1999). **c** Circular dichroism spectrum of CgiPAO (100 μM) in the near-UV/Vis region, expressed in FAD molar ellipticity. **d** Circular dichroism spectrum of GgiPAO (1 μM) in the far-UV region expressed as mean $\Delta\varepsilon$ per residue

Table 2 Kinetic parameters (apparent values) of N^1-acetylSpm and Spm oxidation by CgiPAO

Substrate	k_{cat} (s^{-1})	K_m (μM)	k_{cat}/K_m ($s^{-1}\,M^{-1}$)
N^1-acetylSpm	$19.0 \pm 0.6 \times 10^{-3}$	$3.3 \pm 0.1 \times 10^{1}$	576 ± 23
Spm	$4.6 \pm 1.2 \times 10^{-3}$	$4.4 \pm 1.1 \times 10^{3}$	1.0 ± 0.3

Discussion

Members of the polyamine oxidase gene family have been identified in a wide variety of animals, including vertebrates and invertebrates, as well as in plants and fungi. The CgiPAO displayed a high homology with the molluscan and annelida PAOs retrieved from GenBank and represents a bona fide mollusc polyamine oxidase. In fact, the phylogenetic position of CgiPAO within the lophotrochozoan clade was in agreement with the full-genome evidence proposing the monophyly of lophotrochozoans (Simakov et al. 2013). In addition, multiple sequence alignment revealed a fairly good conservation also with the other invertebrate and plant PAOs, widespread all over the sequence length. Invertebrate PAOs are proposed to be pluripotent enzymes able to oxidase both polyamines and their acetyl derivatives (Polticelli et al. 2012). In this regard, APAO and SMO enzymes are considered to be the result of the vertebrates'

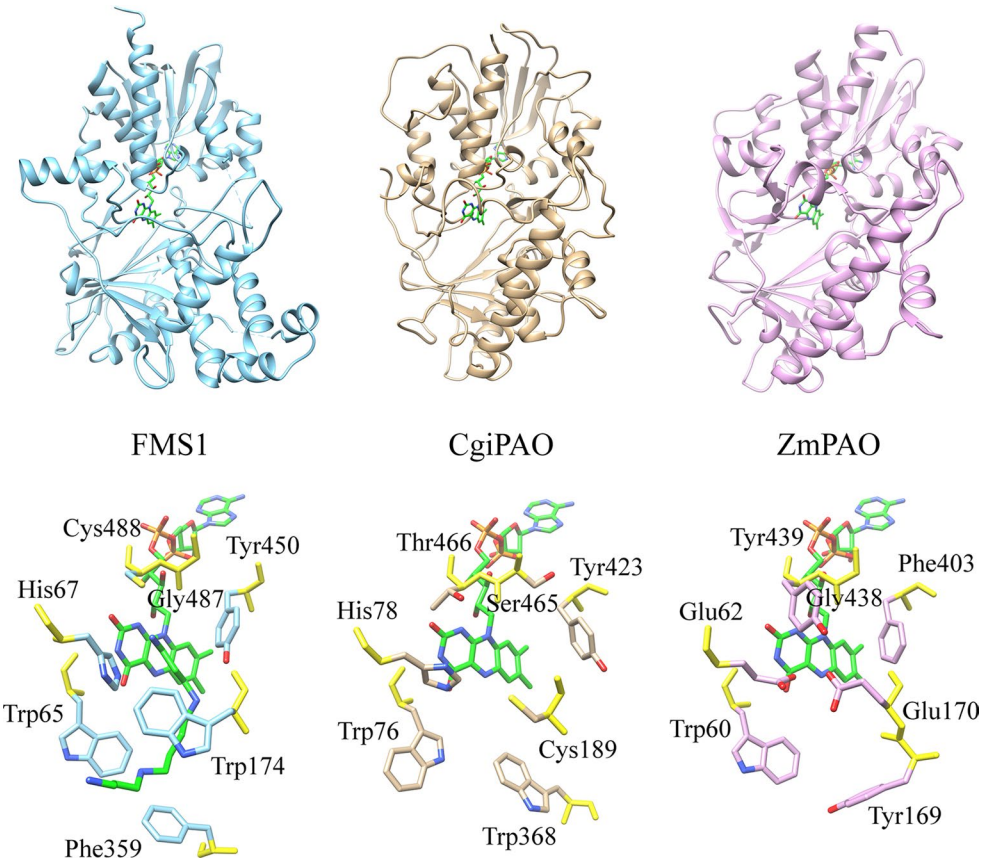

Fig. 5 Comparison of the CgiPAO structural model with Fms1 and ZmPAO three-dimensional structure. *Top* schematic representation of CgiPAO structural model as compared to the three-dimensional structures of Fms1 and ZmaPAO. *Bottom* Structural details of the active site of the three proteins. In the Fms1 active site the substrate Spm is also shown. For clarity FAD and Spm carbon atoms are coloured in *green* (colour figure online)

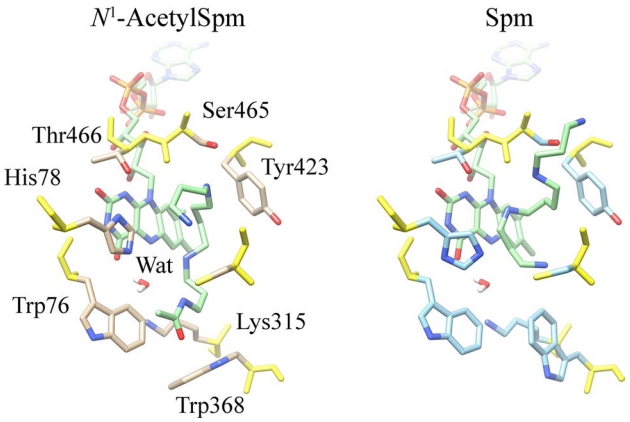

Fig. 6 CgiPAO–substrates complexes obtained by docking simulations. Structural details of the CgiPAO–AcSpm and –Spm complexes obtained by docking simulations. FAD and Spm carbon atoms are coloured in *light green*. See text for details (colour figure online)

specialization of an ancestor PAO protein, following a gene duplication event (Polticelli et al. 2012). To test this hypothesis, the Pacific oyster CgiPAO was cloned, heterologously expressed and biochemical characterized. To the best of our knowledge, no invertebrate PAO has ever been expressed in recombinant form in *E. coli* cells and this is the first report of a molluscan polyamine oxidase overexpressed as a recombinant protein. The analysis of the catalytically active CgiPAO protein reported in this work has shed light on the biochemical features of this enzyme. The purified recombinant enzyme displayed spectroscopic properties typical of PAOs as far as both FAD optical spectrum features and secondary structure content determined by circular dichroism. CgiPAO was able to oxidize both AcSpm and Spm, although the first one has shown to be a better substrate. Docking simulations were in agreement with this finding as both the value of the binding energy and the distance between the substrate C4 atom and the FAD N5 atom were lower in the case of AcSpm, suggesting that the enzyme displayed a higher binding affinity and electron transfer rate for this substrate. From a structural viewpoint, CgiPAO active site showed several features in common with the yeast PAO Fms1. In particular, the presence of Trp76, His78 and Tyr423 was conserved in Fms1 as Trp65, His67 and Tyr450. Worthwhile of note, all animal PAOs/APAOs/SMOs characterized to date, which oxidize the *eso* carbon with respect to the secondary amino group of the substrate, displayed the conservation of a His and a Tyr residue in position orthologous to CgiPAO His78 and Tyr423 (Tavladoraki et al. 2011; Polticelli et al. 2012). Extensive gene duplications have occurred early in

Table 3 Kinetic parameters of selected examples of polyamine oxidases from different organisms

Species	Enzyme	Spm			N^1-acetylSpm			R^a	Ref.
		k_{cat} (s^{-1})	K_m (μM)	k_{cat}/K_m (s^{-1} M^{-1})	k_{cat} (s^{-1})	K_m (μM)	k_{cat}/K_m (s^{-1} M^{-1})		
C. gigas	CgiPAO	4.6×10^{-3}	4,400	1.0	1.9×10^{-2}	33	576	576	b
S. cerevisiae	FMS1	165	10	1.65×10^{7}	47	1.58	2.97×10^{7}	1.8	c
M. musculus	APAO	0.175	716	244	4.5	1.78	2.5×10^{6}	1.0×10^{4}	d
M. musculus	SMO	4.5	90	5×10^{4}	6.8×10^{-2}	800	85	1.7×10^{-3}	e
H. sapiens	SMO	6.6	190	3.47×10^{4}	0.4	492	813	2.3×10^{-2}	f

[a] R is defined as the ratio $[(k_{cat}/K_m)_{AcSpm}]/[(k_{cat}/K_m)_{Spm}]$

[b] This work; 100 mM Tris–HCl buffer (pH 8.5), 25 °C

[c] Landry and Sternglanz 2003; 62.5 mM Tris–HCl buffer (pH 9.0), room temperature

[d] Wu et al. 2003; 50 mM phosphate buffer (pH 7.6), 30 °C

[e] Cervelli et al. 2014b; 100 mM Tris–HCl buffer (pH 8.3), 25 °C

[f] Adachi et al. 2010; 200 mM Tris–HCl buffer (pH 8.3), 25 °C

chordate evolution and whether these duplications were due to complete genome duplication(s) as opposed to segmental or even sequential single gene duplications (Panopoulou et al. 2003) is still matter of debate. In vertebrates' cells, PA catabolism is mediated by the activity of two enzymes, i.e. APAO and SMO, derived by gene duplication, while in invertebrates this biochemical pathway has been proposed to be fulfilled by an ancestor single PAO enzyme (Polticelli et al. 2012). From this viewpoint, comparative analysis of the kinetic properties of Fms1, CgiPAO, APAO and SMO (Table 3), indicates that CgiPAO may represent a first step towards the evolution of specialized PAO enzyme. In fact, *S. cerevisiae* Fms1 shows similar values of k_{cat}/K_m for acetylated and non-acetylated polyamines. The ratio R between the k_{cat}/K_m values (acetylated/non-acetylated) is 1.8. On the contrary, both APAO and SMO from vertebrate (*M. musculus*) are very selective for acetylated polyamines and spermine, respectively (R being about 1.0×10^4 for APAO and 1.7×10^{-3} for SMO; and 2.3×10^{-2} in the case of human SMO). This study showed that CgiPAO was able to catalyse the oxidation of both acetylated and non-acetylated substrates, but the k_{cat}/K_m value was much higher for AcSpm than for Spm. As commented above, this was due to a large difference in K_m values (33 vs 4,400 μM), whereas the k_{cat} values are comparable. The ratio R for *C. gigas* PAO was 576, an intermediate value between 1.8 (Fms1) and 1.0×10^4 (APAO). On the basis of these considerations, it can be postulated that from an ancestral unspecific enzyme, an APAO-like enzyme gradually evolved which, upon gene duplication and further divergence, gave rise in vertebrates to the highly specific APAOs and SMOs. However, further studies on other invertebrate PAOs are needed to confirm this hypothesis. To summarize, the biochemical characterization of the Pacific oyster CgiPAO presented in this work strongly suggests that from yeast to arthropods a single enzyme can satisfy PAs oxidation metabolic need and CgiPAO may represent a typical member of the invertebrate polyamine oxidase family.

Perspectives

The CgiPAO enzyme is a new characterized member of the animal polyamine oxidase gene family and it was expressed for the first time in the *E. coli*. Circular dichroism analysis gave an estimation of the secondary structure content and modelling of the three-dimensional structure of this protein and docking studies highlighted active site features. Nowadays only the crystal structure from yeast Fms1 and maize *Zma* PAOs is available. On the contrary, no tridimensional structure of invertebrate and vertebrate PAOs is known. Despite the huge amount of data on the role played by the vertebrate SMO in PA metabolism, cancer and brain pathologies, many attempts from independent laboratories to obtain SMO protein crystals suitable for X-ray diffraction studies have been made, but were unsuccessful (Tavladoraki et al. 2011). The CgiPAO could represent a novel enzyme to challenge the PAO crystal structure, considering that the smaller size of this protein with respect to the vertebrate SMO could be very promising. The disposal of this pluripotent enzyme can have as well multiple applications in biotechnology and pharmaceutical fields, including anticancer therapy. In fact, in the last decade an increasing interest has been focused on the exploitation of the human SMO and BSAO enzyme activities in antitumoral treatment, since Spm catabolic degradation is closely related to DNA oxidation and apoptosis, mainly via H_2O_2 production (Agostinelli et al. 2007, 2009; Amendola et al. 2009, 2013, 2014; Cervelli et al. 2014a). In particular, it has been demonstrated that the release of toxic Spm metabolites (H_2O_2

and aldehydes) into melanoma, wild-type and multidrug resistant cells, after treatment with BSAO-catalysed oxidation of Spm, can induce inhibition of tumour growth (Agostinelli et al. 2009). Analogously, it might be conceived that CgiPAO, immobilized in a biocompatible polymer, could be utilized for anticancer therapeutic setting as a new and broader enzyme tool when combined with both Spm and acetyl derivatives, to produce the slow release of H_2O_2 and aldehydes at such concentration that induces tumour cell death by apoptosis rather than necrosis. In conclusion, the toxic enzymatic oxidation products generated by CgiPAO could be utilized in a combined treatment with drugs currently used in therapy and/or compounds with lysosomotropic properties, and hyperthermia associated with irradiation (Agostinelli et al. 2009; Amendola et al. 2013, 2014), to selectively generate reactive oxygen species in cancer cells.

Acknowledgments We wish to thank the University of Roma Tre for financial support and Prof. Marco Oliverio (Sapienza University of Rome, Italy) for useful discussion.

Conflict of interest The authors declare that they have no conflict of interest.

References

Adachi MS, Juarez PR, Fitzpatrick PF (2010) Mechanistic studies of human spermine oxidase: kinetic mechanism and pH effects. Biochemistry 49:386–392

Agostinelli E, Arancia G, Dalla Vedova L, Belli F, Marra M, Salvi M, Toninello A (2004) The biological functions of polyamine oxidation products by amine oxidises: perspectives of clinical applications. Amino Acids 27:347–358

Agostinelli E, Tempera G, Molinari A, Salvi M, Battaglia V, Toninello A, Arancia G (2007) The physiological role of biogenic amines redox reactions in mitochondria. New perspectives in cancer therapy. Amino Acids 33:175–187

Agostinelli E, Condello M, Tempera G, Macone A, Bozzuto G, Ohkubo S, Calcabrini A, Arancia G, Molinari A (2009) The combined treatment with chloroquine and the enzymatic oxidation products of spermine overcomes multidrug resistance of melanoma M14 ADR2 cells: a new therapeutic approach. Int J Oncol 45:1109–1122

Aliverti A, Curti B, Vanoni MA (1999) Identifying and quantitating FAD and FMN in simple and iron–sulfur-containing flavoproteins. Met Mol Biol 131:9–23

Amendola R, Cervelli M, Fratini E, Polticelli F, Sallustio DE, Mariottini P (2009) Spermine metabolism and anticancer therapy. Curr Cancer Drug Targets 9:118–130

Amendola R, Cervelli M, Fratini E, Sallustio DE, Tempera G, Ueshima T, Mariottini P, Agostinelli E (2013) Reactive oxygen species spermine metabolites generated from amine oxidases and radiation represent a therapeutic gain in cancer treatments. Int J Oncol 43:813–820

Amendola R, Cervelli M, Tempera G, Fratini E, Varesio L, Mariottini P, Agostinelli E (2014) Spermine metabolism and radiation-derived reactive oxygen species for future therapeutic implications in cancer: an additive or adaptive response. Amino Acids 46:487–498

Andrade MA, Chacón P, Merlo JJ, Morán F (1993) Evaluation of secondary structure of proteins from UV circular dichroism using an unsupervised learning neural network. Prot Eng 6:383–390

Bellelli A, Cavallo S, Nicolini L, Cervelli M, Bianchi M, Mariottini P, Zelli M, Federico R (2004) Mouse spermine oxidase: a model of the catalytic cycle and its inhibition by N, N1-bis(2,3-butadienyl)-1,4-butanediamine. Biochem Biophys Res Commun 322:1–8

Bianchi M, Amendola R, Federico R, Polticelli F, Mariottini P (2005) Two short protein domains are responsible for the nuclear localization of mouse spermine oxidase (mSMO)μ isoform. FEBS J 272:3052–3059

Bianchi M, Polticelli F, Ascenzi P, Botta M, Federico R, Mariottini P, Cona A (2006) Inhibition of polyamine and spermine oxidases by polyamine analogues. FEBS J 273:1115–1123

Binda C, Coda A, Angelini R, Federico R, Ascenzi P, Mattevi A (1999) A 30-angstrom-long U-shaped catalytic tunnel in the crystal structure of polyamine oxidase. Structure 7:265–276

Bradford MM (1976) A rapid and sensitive method for the quantitation of microgram quantities of protein utilising the principle of protein-dye binding. Anal Biochem 72:248–254

Capone C, Cervelli M, Angelucci E, Colasanti M, Macone A, Mariottini P, Persichini T (2013) A role for spermine oxidase as a mediator of reactive oxygen species production in HIV-Tat-induced neuronal toxicity. Free Radic Biol Med 63:99–107

Casero RA Jr, Marton LJ (2007) Targeting polyamine metabolism and function in cancer and other hyperproliferative diseases. Nat Rev Drug Disc 6:373–390

Cervelli M, Polticelli F, Federico F, Mariottini P (2003) Heterologous expression and characterization of mouse spermine oxidase. J Biol Chem 278:5271–5276

Cervelli M, Bellini A, Bianchi M, Marcocci L, Nocera S, Polticelli F, Federico R, Amendola R, Mariottini P (2004) Mouse spermine oxidase gene splice variants. Nuclear subcellular localization of a novel active isoform. Eur J Biochem 271:760–770

Cervelli M, Bellavia G, Fratini E, Amendola R, Polticelli F, Barba M, Federico R, Signore F, Gucciardo G, Grillo R, Woster PM, Casero RA Jr, Mariottini P (2010) Spermine oxidase (SMO) activity in breast tumor tissues and biochemical analysis of the anticancer spermine analogues BENSpm and CPENSpm. BMC Cancer 10:555

Cervelli M, Amendola R, Polticelli F, Mariottini P (2012) Spermine oxidase: ten years after. Amino Acids 42:441–450

Cervelli M, Salvi D, Polticelli F, Amendola R, Mariottini P (2013a) Structure-function relationships in the evolutionary framework of spermine oxidase. J Mol Evol 76:365–370

Cervelli M, Bellavia G, D'Amelio M, Cavallucci V, Moreno S, Berger J, Nardacci R, Marcoli M, Maura G, Piacentini M, Amendola R, Cecconi F, Mariottini P (2013b) A new transgenic mouse model for studying the neurotoxicity of spermine oxidase dosage in the response to excitotoxic injury. PLoS One 8:e64810

Cervelli M, Angelucci E, Germani F, Amendola R, Mariottini P (2014a) Inflammation, carcinogenesis and neurodegeneration studies in transgenic animal models for polyamine research. Amino Acids 46:521–530

Cervelli M, Angelucci E, Stano P, Leboffe L, Federico R, Antonini G, Mariottini P, Polticelli F (2014b) The Glu216/Ser218 pocket is a major determinant of spermine oxidase substrate specificity. Biochem J 461:453–459

Chen SH, Su SY, Lo CZ, Chen KH, Huang TJ, Kuo BH, Lin CY (2009) PALM: a paralleled and integrated framework for phylogenetic inference with automatic likelihood model selectors. PLoS One 4:e8116

Deleage G, Geourjon C (1993) An interactive graphic program for calculating the secondary structure-content of proteins from circular-dichroism spectrum. Comput Appl Biosci 9:197–199

Edmonson DE, Tollin G (1971) Circular dichroism studies of the flavin chromophore and of the relation between redox properties and flavin environment in oxidases and dehydrogenases. Biochemistry 10:113–124

Huang Q, Liu Q, Hao Q (2005) Crystal structures of Fms1 and its complex with spermine reveal substrate specificity. J Mol Biol 348:951–959

Laemmli UK (1970) Cleavage of structural proteins during assembly of the head of bacteriophage T4. Nature 277:680–685

Landry J, Sternglanz R (2003) Yeast Fms1 is a FAD-utilizing polyamine oxidase. Biochem Biophys Res Commun 303:771–776

Larkin M, Blackshields G, Brown N, Chenna R, McGettigan P, McWilliam H, Valentin F, Wallace I, Wilm A, Lopez R, Thompson J, Gibson T, Higgins D (2007) Clustal W and Clustal X version 2.0. Bioinformatics 23:2947–2948

McIntire WS, Hartman C (1993) In: Davison VL (ed) Principle and application of quinoproteins. Marcel Dekker Inc., New York, pp 97–171

Panopoulou G, Hennig S, Groth D, Krause A, Poustka AJ, Herwig R, Vingron M, Lehrach H (2003) New evidence for genome-wide duplications at the origin of vertebrates using an amphioxus gene set and completed animal genomes. Genome Res 13:1056–1066

Polticelli F, Basran J, Faso C, Cona A, Minervini G, Angelini R, Federico R, Scrutton N, Tavladoraki P (2005) Biochemistry 44:16108–16120

Polticelli F, Salvi D, Mariottini P, Amendola R, Cervelli M (2012) Molecular evolution of the polyamine oxidase gene family in Metazoa. BMC Evol Biol 12:90

Ronquist F, Teslenko M, van der Mark P, Ayres D, Darling A, Höhna S, Larget B, Liu L, Suchard MA, Huelsenbeck JP (2012) MrBayes 3.2: efficient Bayesian phylogenetic inference and model choice across a large model space. Syst Biol 61:539–542

Roy A, Kucukural A, Zhang Y (2010) I-TASSER: a unified platform for automated protein structure and function prediction. Nat Protoc 5:725–738

Sambrook J, Fritsch EF, Maniatis T (1989) Molecular cloning: a laboratory manual, 2nd edn. Cold Spring Harbor Laboratory Press, Cold Spring Harbor

Simakov O, Marletaz F, Cho SJ, Edsinger-Gonzales E, Havlak P, Hellsten U, Kuo DH, Larsson T, Lv J, Arendt D, Savage R, Osoegawa K, de Jong P, Grimwood J, Chapman JA, Shapiro H, Aerts A, Otillar RP, Terry AY, Boore JL, Grigoriev IV, Lindberg DR, Seaver EC, Weisblat DA, Putnam NH, Rokhsar DS (2013) Insights into bilaterian evolution from three spiralian genomes. Nature 493:526–531

Sreerama N, Woody RW (2000) Estimation of protein secondary structure from circular dichroism spectra: comparison of CONTIN, SELCON and CDSSTR methods with an expand reference set. Anal Biochem 287:252–260

Tavladoraki P, Cervelli M, Antonangeli F, Minervini G, Stano P, Federico R, Mariottini P, Polticelli F (2011) Probing mammalian spermine oxidase enzyme–substrate complex through molecular modeling, site-directed mutagenesis and biochemical characterization. Amino Acids 840:1115–1126

Thomas T, Thomas TJ (2001) Polyamines in cell growth and cell death: molecular mechanisms and therapeutic applications. Cell Mol Life Sci 2:244–258

Trott O, Olson AJ (2010) AutoDock Vina: improving the speed and accuracy of docking with a new scoring function, efficient optimization and multithreading. J Comput Chem 31:455–461

Van den Munckhof RJ, Denyn M, Tigchelaar-Gutter W, Schipper RG, Verhofstad AAJ, Van Noorden CJF, Frederiks WM (1995) *In situ* substrate specificity and ultrastructural localization of polyamine oxidase activity in unfixed rat tissues. J Histochem Cytochem 43:1155–1162

Wallace HM, Fraser AV, Hughes A (2003) A perspective of polyamine metabolism. Biochem J 376:1–14

Waterhouse A, Procter J, Martin D, Clamp M, Barton G (2009) Jalview version 2–a multiple sequence alignment editor and analysis workbench. Bioinformatics 25:1189–1191

Wu T, Yankovskaya V, William S, McIntire W (2003) Cloning, sequencing, and heterologous expression of the murine peroxisomal flavoprotein, *N*1-acetylated polyamine oxidase. J Biol Chem 278:20514–20525

Xu D, Zhang J, Roy A, Zhang Y (2011) Automated protein structure modeling in CASP9 by I-TASSER pipeline combined with QUARK-based ab initio folding and FG-MD-based structure refinement. Proteins 79(S10):147–160

Zhang G, Fang X, Guo X, Li L, Luo R, Xu F, Yang P, Zhang L, Wang X, Qi H, Xiong Z, Que H, Xie Y, Holland PW, Paps J, Zhu Y, Wu F, Chen Y, Wang J, Peng C, Meng J, Yang L, Liu J, Wen B, Zhang N, Huang Z, Zhu Q, Feng Y, Mount A, Hedgecock D, Xu Z, Liu Y, Domazet-Loso T, Du Y, Sun X, Zhang S, Liu B, Cheng P, Jiang X, Li J, Fan D, Wang W, Fu W, Wang T, Wang B, Zhang J, Peng Z, Li Y, Li N, Wang J, Chen M, He Y, Tan F, Song X, Zheng Q, Huang R, Yang H, Du X, Chen L, Yang M, Gaffney PM, Wang S, Luo L, She Z, Ming Y, Huang W, Zhang S, Huang B, Zhang Y, Qu T, Ni P, Miao G, Wang J, Wang Q, Steinberg CE, Wang H, Li N, Qian L, Zhang G, Li Y, Yang H, Liu X, Wang J, Yin Y, Wang J (2012) The oyster genome reveals stress adaptation and complexity of shell formation. Nature 490:49–54